Chemical Science

ROYAL SOCIETY OF CHEMISTRY

EDGE ARTICLE

View Article Online
View Journal | View Issue

Cite this: *Chem. Sci.*, 2026, **17**, 1223

All publication charges for this article have been paid for by the Royal Society of Chemistry

Received 22nd September 2025
Accepted 14th November 2025

DOI: 10.1039/d5sc07328f

rsc.li/chemical-science

A radical strategy to the synthesis of bicyclo[1.1.1]pentyl *C*-glycosides

Giulio Goti, *[a] Alessia Marrese, †[a] Simone Baldon, †[a] Patricia Gómez Roibás, [ab] Giorgio Pelosi, [c] Andrea Sartorel [a] and Luca Dell'Amico *[a]

Aryl *C*-glycosides, in which carbohydrates are directly linked to aryl fragments through a stable C–C bond, are an important class of biologically active molecules widely found in nature. These compounds exhibit resistance to (enzymatic) hydrolysis, a property that has been successfully leveraged in the development of metabolically stable drugs. On the other hand, despite their potential, three-dimensional analogues of aryl *C*-glycosides remain largely overlooked. Here, we present a three-component radical strategy that grants access to this underexplored chemical space. Specifically, glycosyl bromides serve as a source of glycosyl radicals, which can react with [1.1.1]propellane and a suitable SOMOphile to afford bicyclopentyl *C*-glycosides. These C(sp^3)-rich analogues replace a planar aryl ring with a three-dimensional bicyclopentyl moiety, which is expected to enhance physicochemical properties. The protocol is practical, mild, and amenable to scalable synthesis in continuous flow. Experimental and computational studies support a radical chain mechanism under kinetic control.

Introduction

Aryl *C*-glycosides are important compounds encompassing structurally diverse natural products and drugs.[1] The distinctive feature of these molecules – *i.e.* the presence of a stable C–C bond connecting a saccharide unit to an aryl moiety – confers resistance towards hydrolytic enzymes, which makes them privileged glycomimetic candidates in drug development programs (Scheme 1a).[2] Given their relevance, numerous synthetic methods for the efficient preparation of aryl *C*-glycosides have been developed in recent years, most of them achieving the formation of the aryl *C*-glycoside linkage through cationic, anionic, and radical glycosyl intermediates, or with the use of transition metal catalysts.[1b,3]

On the other hand, the replacement of planar conjugated moieties with three-dimensional fragments has been established as a potent strategy in medicinal chemistry to improve the physicochemical properties of lead compounds and increase their success rate in clinical trials.[4] Driven by this principle, in the past few years synthetic chemists have focused on the development of C(sp^3) rich bioisosteres able to replace planar aromatic cores, which are highly represented motifs in drugs.[5] Among these, the saturated bicyclo[1.1.1]pentane (BCP) is arguably the most studied bioisostere of phenyl rings.[6] When 1,3-disubstituted at the bridgehead positions, this core acts as

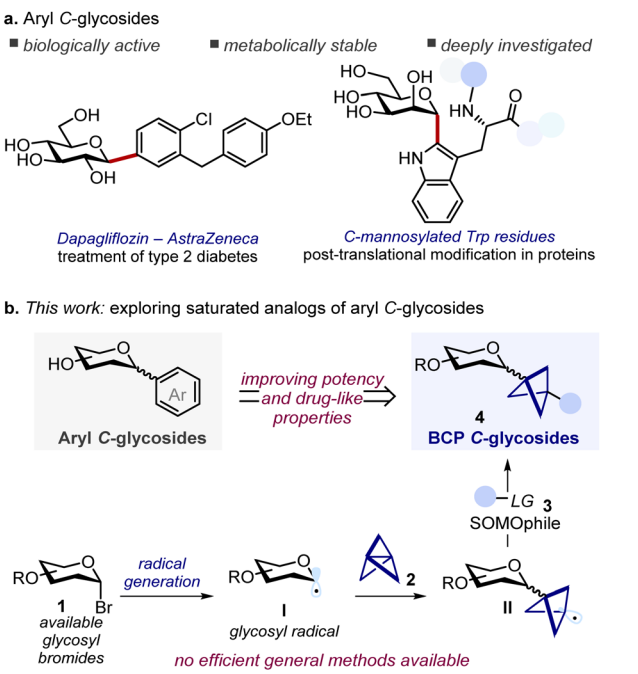

Scheme 1 (a) Representative examples of aryl *C*-glycosides as natural products and drugs. (b) Three-component radical approach towards bicyclo[1.1.1]pentyl (BCP) *C*-glycosides as saturated analogs. Trp: tryptophan; LG: leaving group; SOMO: singly occupied molecular orbital; BCP: bicyclo[1.1.1]pentyl.

[a]*Department of Chemical Sciences, University of Padova, Via Francesco Marzolo 1, 35131 Padova, Italy. E-mail: giulio.goti@unipd.it; luca.dellamico@unipd.it*

[b]*Centro Singular de Investigación en Química Biolóxica e Materiais Moleculares (CiQUS), Universidade de Santiago de Compostela, 15782 Santiago de Compostela, Spain*

[c]*Department of Chemistry, Life Sciences and Environmental Sustainability, University of Parma, Parco Area delle Scienze 17, 43124 Parma, Italy*

† These authors contributed equally.

a rigid spacer projecting the substituents with exit vectors at approximately 180° that well mimic the spatial arrangement of *para*-disubstituted arenes. As such, bioisosteric replacement strategies with BCPs have been successfully applied in drug discovery programs, allowing the preparation of saturated analogs with unaltered targeting ability that show improved potency or enhanced physicochemical properties (*e.g.* solubility, and metabolic stability), and that can enable patent circumvention.[7]

Despite their potential, the development of saturated analogues of aryl *C*-glycosides has remained largely underdeveloped, which precludes the study of their properties and implementation in drug development campaigns. A possible explanation for this synthetic gap is the paucity of methods for the introduction of highly three-dimensional fragments at the anomeric position of saccharides. Indeed, while *C*-glycosylation strategies for the functionalization with alkyl, alkenyl, and alkynyl groups are well developed (either *via* polar or radical chemistry),[3b,d,8] these approaches are mainly limited to the instalment of linear flexible carbon chains that do not have the requisites to properly mimicking the defined exit vectors provided by rigid aromatic scaffolds.

Restricting our focus to saturated *C*-glycosides featuring a BCP unit directly linked to the anomeric position, we envisioned that this moiety could be conveniently introduced by functionalization of [1.1.1]propellane (Scheme 1b).[9] This strained precursor exhibits omniphilic reactivity, being able to react with electrophiles, strong nucleophiles, and radicals. Notably, radical addition to [1.1.1]propellane proceeds under remarkably mild conditions,[10] making it particularly suited for functionalizing complex substrates such as glycosides.[3d,11] In this regard, rare preparations of BCP *C*-glycosides have been independently reported by the Anderson and Molander groups by ring opening of [1.1.1]propellane with glycosyl radicals,[10n,o] although both protocols involve the use of either unstable radical precursors (*e.g.* glycosyl iodides), transition metal-based photocatalysts, or expensive SOMOphiles (*e.g.* Suginome reagent). Notably, although these methods targeted a broad range of alkyl iodide and bromide substrates, their application to *C*-glycosyl derivatives was limited. Both reported just a single glucoside derivative and, in one case, with an unusual β-stereoselectivity that we believe misassigned. Furthermore, the scalability and further derivatization of the *C*-glycoside products were not investigated. With this work we aim to address these limitations providing a general versatile strategy to the efficient synthesis of BCP *C*-glycosides to enable their study and characterization.[12]

Taking inspiration from the work of the Molander group, we recognized that readily available glucosyl bromide **1** could serve as a radical precursor to glycosyl radical **I**. This reactive intermediate would then engage in a radical addition to [1.1.1]propellane **2** giving the BCP radical **II**.[10n,o] Finally, reaction with a suitable SOMOphile **3** would deliver the desired BCP *C*-glycoside **4** (Scheme 1b). We reasoned that careful selection of the SOMOphile **3** would be key to the success of this three-component radical approach. Here, two key challenges must be considered: (i) glycosyl radical **I** has to discriminate between propellane **2** and SOMOphile **3**, leading to the selective formation of the key intermediate **II**; (ii) **II** must then react selectively with SOMOphile **3** over propellane **2**, thus preventing staffane side-products. Herein we detail our efforts in implementing this strategy to provide general and efficient access to saturated aryl *C*-glycoside analogs. Two distinct protocols for the hydroglycosylation and carboboration of [1.1.1]propellane were developed, providing synthetically useful sugar-based building blocks that enabled smooth diversification into a small library of BCP *C*-glycoside derivatives. A thorough mechanistic investigation is also presented.

Results and discussion

Strategy validation – hydroglycosylation of propellanes

To test the feasibility of our approach, we began investigating the model reaction between acetobromo-α-D-glucose **1a** (0.1 mmol), [1.1.1]propellane **2a**, and tris(trimethylsilyl)silane **3a** (Table 1).[13] After optimization (for details, see SI, Section C.1) we found that using a slight excess of both propellane **2a** and silane **3a** (1.5 equiv.), along with 4CzIPN as photocatalyst (PC)[14] under blue LED ($\lambda_{max} = 427$ nm) irradiation provided BCP *C*-glucoside **4a** in good yield and stereoselectivity (71% yield; α:β, 7 : 1) as judged by ^{1}H NMR analysis of the crude mixture (Table 1, entry 1), while minimizing the formation of staffane **5a** and 1-deoxyglucoside **6a** (9% and 20% yield, respectively). Notably, we found that the use of trialkylamines as hydrogen atom donors suppressed the formation of the reduced side-product **6a**, although product **4a** was obtained in diminished yield and with substantial formation of staffane **5a** (Table 1, entries 2,3). Since this latter side-product is particularly difficult to purify by flash column chromatography from the desired *C*-glycoside **4a**, we selected silane **3a** as the best hydrogen atom transfer (HAT) donor species. Stoichiometry was also found to be a key parameter, as increasing the excess of either propellane **2a** and silane **3a** led to decreased performance (Table 1, entries 4–6). Pleasingly, only a slight decrease in yield was observed when performing the reaction on a 0.2 mmol scale (63% yield, Table 1, entry 7). Finally, control experiments revealed that the reaction can also proceed in the absence of the PC and light, albeit with lower efficiency and increased side-products formation (Table 1, entries 8–10). These results indicate that a radical chain reaction can be thermally initiated, although the process is relatively inefficient and the use of 4CzIPN as photoinitiator is beneficial.

With the best conditions in hand, we sought to evaluate the applicability and generality of this three-component hydroglycosylation protocol (Table 2). First, we demonstrated that the protocol is scalable to a 2 mmol reaction under batch conditions, giving **4a** in 42% yield after isolation (336 mg). Then, we varied the protecting groups of D-glucosyl bromide showing that benzoyl and pivaloyl esters are also well tolerated (**4b–c**). To our delight, the reaction was amenable to the functionalization of several hexoses, pentoses, and deoxysugars in their pyranosidic form, enabling the preparation of BCP *C*-glycosides of D-galactose, D-mannose, D-lyxose, L-rhamnose, and L-fucose in moderate to good yields and excellent a stereoselectivity (**4d–h**). A fluorinated D-galactose derivative was found to be a competent

Table 1 Optimization of the reaction conditions[a]

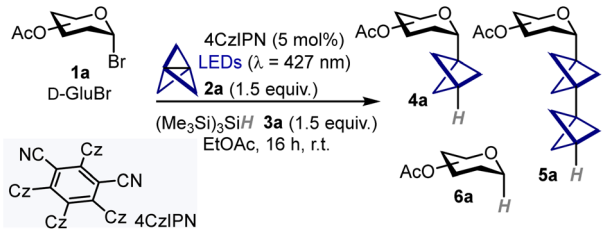

Entry	Deviation from standard conditions	4a[b] (%)	5a[b] (%)	6a[b] (%)
1	—	**71**	**9**	**20**
2	iPr_2EtN instead of $(Me_3Si)_3SiH$	33	28	—
3	Et_3N instead of $(Me_3Si)_3SiH$	37	17	—
4	3 equiv. of **2a**	48	24	23
5	3 equiv. of **3a**	53	11	36
6	3 equiv. of **2a** and **3a**	59	11	28
7	0.2 mmol	63	7	30
8	No 4CzIPN	44	8	45
9	No light	34	13	48
10	No PC, no light, 40 °C	40	18	21

[a] Reactions were performed using 0.1 mmol of **1a**, [1.1.1]propellane **2a** as solution in Et_2O, and 0.4 mL of EtOAc. [b] Determined by ^1H NMR analysis of the crude mixture using trichloroethylene as the internal standard. 4CzIPN: 1,2,3,5-tetrakis(carbazol-9-yl)-4,6-dicyanobenzene; Cz: carbazoyl; LED: light-emitting diode; r.t.: room temperature.

substrate (**4i**), showcasing the suitability of the method for the preparation of innovative chemical probes.[15] When [3.1.1]propellane **2b** was used we successfully obtained *C*-glucoside **4j** whose bicycloheptyl moiety mimics a *meta*-disubstituted arene, albeit the reaction occurred in somewhat decreased yield.[16] Finally, disaccharides bearing either a 1,4-α and 1,4-β glycosidic linkage gave the corresponding products **4k,l** in synthetically useful yields. Remarkably, all products were generally obtained as the α anomers with very high levels of stereoselectivity. In all cases, BCP *C*-glycosides **4** were formed as the major products, along with traces of staffanes **5** and minor formation of 1-deoxyglycosides **6**, as judged by ^1H NMR analysis of crude reaction mixtures.

Carboboration of [1.1.1]propellane towards BCP *C*-glycoside boronates

Next, we wondered whether this radical strategy could be expanded to other classes of SOMOphiles to access BCP *C*-glycosides of increased synthetic value. To our delight, after intense screening and optimization of key parameters we identified diboron(4) reagents as suitable reaction partners (for details see SI, Section C.2).[10o,17] Specifically, we found that glycosyl bromides **1** react in presence of an excess of [1.1.1]propellane **2a** and bis(1,3-propanediolate)diboron (B_2pro_2) **3b** to give BCP *C*-glycoside boronates **7** with good yield and good to excellent stereoselectivity (Table 3). Notably, this reaction occurs under thermal conditions – *i.e.*, in the absence of light or PC – with perfect selectivity for boronate **7**. Since isolation by flash chromatography proved unsuccessful due to degradation on silica gel, the Bpro moiety was instrumental, as it could be smoothly converted into the corresponding MIDA ester **8**, enabling purification and full characterization.[18] This protocol could be applied to both peracetylated and perbenzoylated glucosides (**8a,b**) as well as a variety of hexo- and pentopyranoses (**8c–8f**) (Table 3). While these boronates were generally obtained with good to excellent stereoselectivity for the α anomer, a lower α : β ratio of 2 : 1 was observed for D-xylose derivative **8e**, likely due to its higher conformational freedom.[19] Deoxy sugars from the L-series also reacted well (**8g,h**). This enabled us to grow crystals suitable for X-ray analysis of the L-fucose derivative **8h**, confirming the α configuration of the anomeric center and determining key structural parameters within the BCP moiety (see SI, Section E). Finally, we were able to successfully apply the protocol to a fluoro D-galacto derivative (**8i**) and to D-maltose and D-lactose disaccharides (**8j,k**).

Table 2 Light-driven hydroglycosylation of propellanes[a]

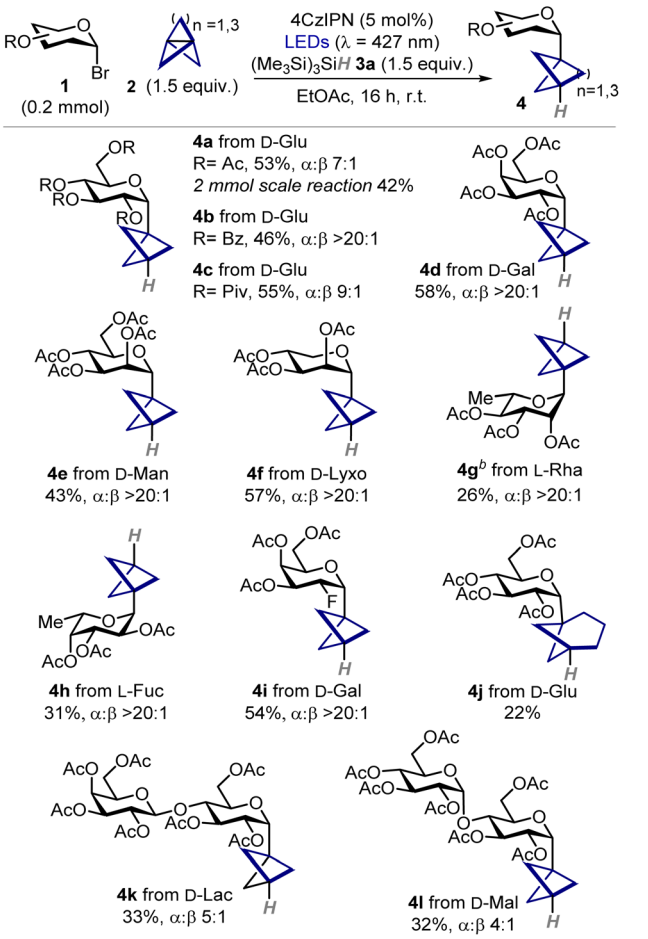

[a] Reactions performed on a 0.2 mmol scale using 4CzIPN (5 mol%), propellane **2** as solution in Et_2O (1.5 equiv.), and $(Me_3Si)_3SiH$ **3a** (1.5 equiv.). Yields refer to isolated products **4**. α:β ratios were determined by ^1H NMR analysis of the crude mixture using trichloroethylene as the internal standard. [b] Reaction performed at 0.3 mmol scale. 4CzIPN: 1,2,3,5-tetrakis(carbazol-9-yl)-4,6-dicyanobenzene; LED: light-emitting diode; r.t.: room temperature.

Continuous flow scale-up and derivatization studies

To explore the synthetic potential of BCP *C*-glycosyl boronates, we scaled up the synthesis of glucoside **8a** and took advantage of the boronate group as a handle for further diversification.[20] Initial attempts to increase the reaction scale under batch conditions resulted in poor conversions due to slower kinetics. However, adapting the process to continuous flow using a homemade reactor enabled us to perform the reaction on a 2.0 mmol scale without loss of efficiency (see SI, Section F.2).[21] Notably, the use of B_2pro_2 was crucial, as it ensured complete solubility of the reaction mixture, thereby facilitating a smooth transition to flow conditions. Finally, transesterification with MIDA afforded glucosyl boronate **8a** in 54% overall yield (Scheme 2).

While treating crude boronate **7** with oxone smoothly provides access to tertiary alcohol **9** (45% yield over two steps), MIDA ester **8a** could be efficiently converted into the corresponding tetrafluoroborate salt **10** (93% yield) (Scheme 2). Pleasingly, this key radical source participated in a Cu-catalyzed metallaphotoredox Chan–Lam reaction with 6-chloroindole, giving the corresponding C–N cross-coupled product **11**.[10o] Alternatively, **10** could also be employed in a Giese-type addition to dimethyl fumarate (**12**), and to methyl vinyl ketone when using a Cu(I) salt as a co-catalyst (**13**).[22] Finally, a Ni-catalyzed metallaphotoredox protocol enabled the forging of a C(sp^3)–C(sp^2) bond, affording the cross-coupled product **14**.[17d]

Mechanistic investigation

After having assessed the generality of the developed methods, we aimed to elucidate the involved reaction mechanisms, starting from the hydroglycosylation protocol (Scheme 3a).

To gather insights on a possible thermal initiation pathway, we first studied the behavior of [1.1.1]propellane **2a** upon mixing it with silane $(Me_3Si)_3SiH$ **3a.** Interestingly, we found that these two species can react together to give the addition product **15**, a compound that could also be identified as side-product in the model reaction crude mixture. This addition reaction is completely inhibited in the presence of TEMPO (2,2,6,6-tetramethyl-1-piperidinyloxy) and a TEMPO adduct strongly support the involvement of silyl radicals (for details see SI, Section G).

Along this line, when the model reaction was performed in the presence of TEMPO, the formation of the BCP *C*-glycoside **4a** was also completely suppressed, further supporting the radical nature of the transformation. A ^{2}H-labelling experiment performed using the deuterated silane **3a**-d_1 resulted in the formation of glycoside **4a** with 50% deuterium incorporation (as judged by ^{1}H NMR), which unequivocally demonstrated the role of $(Me_3Si)_3SiH$ **3a** as HAT donor. Based on these findings, we propose the following mechanism for the hydroglycosylation reaction (Scheme 3a bottom). A main initiation pathway involves the oxidation of silane **3a** (E_{ox} ($(Me_3Si)_3SiH^{\bullet+}/(Me_3Si)_3$-SiH) = +0.73 V *vs.* SCE in CH_3CN)[23] from the photoexcited 4CzIPN* ($E_{red}^{1/2}$ ($PC^*/PC^{\bullet-}$) = +1.43 V *vs.* SCE in CH_3CN),[14b] which upon deprotonation leads to the formation of silyl radical

Table 3 Carboboration of [1.1.1]propellane with glycosyl bromides[a]

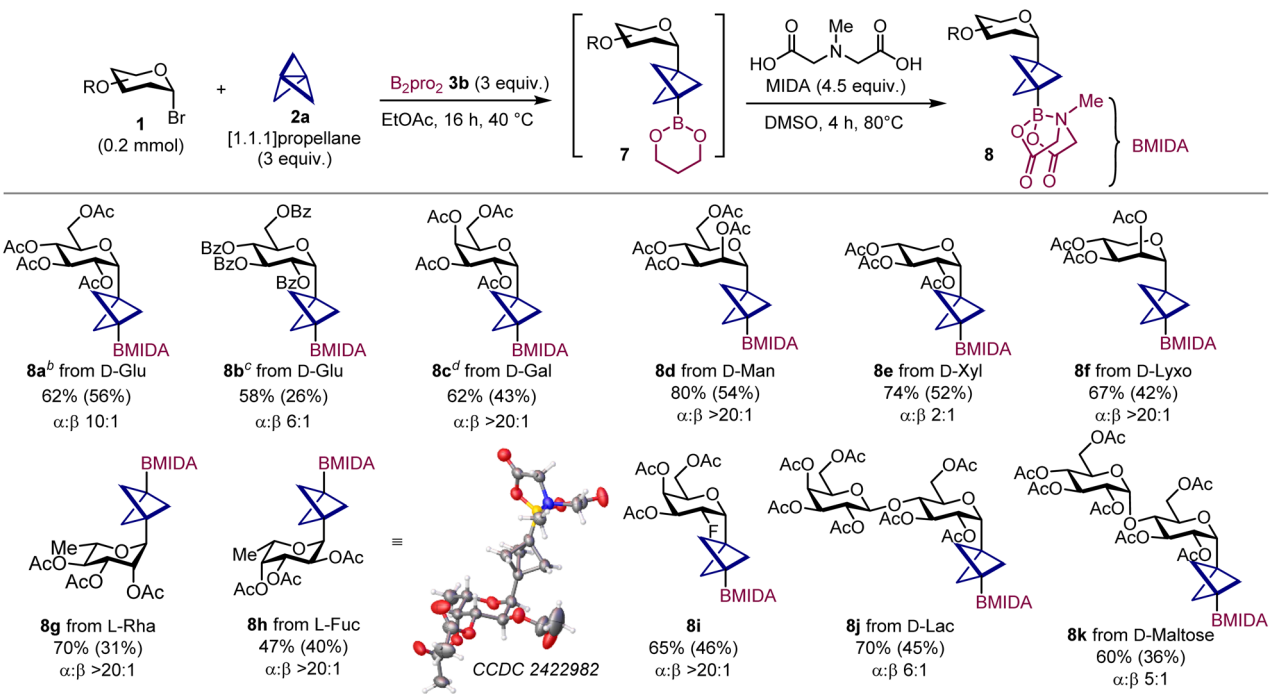

[a] Reactions performed on a 0.2 mmol scale using [1.1.1]propellane **2** as solution in Et_2O (3.0 equiv.), and B_2pro_2 **3b** (3.0 equiv.). Yields outside brackets refer to **7** as determined by ^{1}H NMR. Yields in brackets refer to isolated products **8**. α : β ratios were determined by ^{1}H NMR analysis of the crude mixture using trichloroethylene as the internal standard. [b] Carboboration run for 2 h. [c] Carboboration run for 5 h. [d] Reaction run using 4 equiv. of both **2a** and B_2pro_2. B_2pro_2: bis(1,3-propanediolate)diboron; MIDA: *N*-methyliminodiacetic acid.

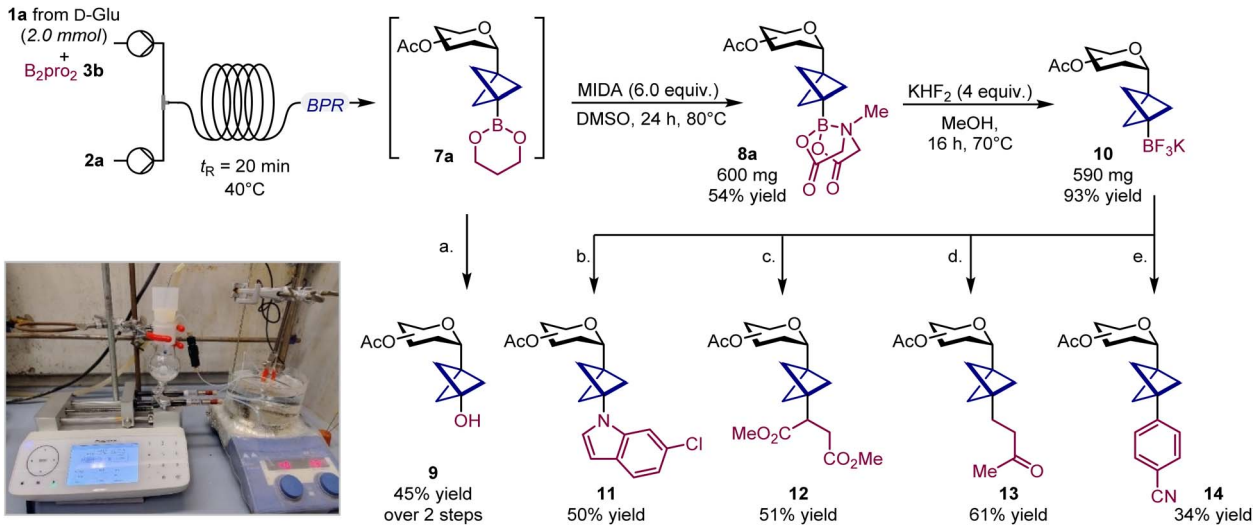

Scheme 2 Reaction scale-up and product derivatization. Scale up performed on 2.0 mmol scale using [1.1.1]propellane **2a** as solution in Et_2O (3.0 equiv.), and B_2pro_2 **3b** (3.0 equiv.). Yields refer to isolated products. (a) Oxone (10 equiv.), K_3PO_4 (3 equiv.), H_2O (5 equiv.), THF, 50 °C. (b) **10** (2 equiv.), 6-chloroindole (1 equiv.), $Ir[dF(CF_3)ppy]_2(bpy)PF_6$ (2 mol%), $Cu(acac)_2$ (50 mol%), Cs_2CO_3 (3 equiv.), LEDs $\lambda = 456$ nm, 1,4-dioxane. (c) **10** (1 equiv.), $Ir[dF(CF_3)ppy]_2(bpy)PF_6$ (2 mol%), $Na_2HPO_4 \cdot 2H_2O$ (3 equiv.), dimethyl fumarate (1.5 equiv.), LEDs $\lambda = 456$ nm, THF. **12** was obtained as a mixture with 1 : 1 d.r. (d) **10** (1 equiv.), $Ir[dF(CF_3)ppy]_2(bpy)PF_6$ (2 mol%), $Na_2HPO_4 \cdot 2H_2O$ (3 equiv.), $Cu(CH_3CN)_4BF_4$ (12.5 mol%), methyl vinyl ketone (1.5 equiv.), LEDs $\lambda = 456$ nm, THF. (e) $Ir[dF(CF_3)ppy]_2(dtbpy)PF_6$ (5 mol%), 4-bromobenzonitrile (1 equiv.), **10** (1.5 equiv.), Na_2CO_3 (2 equiv.), $Ni(dtbpy)_2Br_2$ (10 mol%), LEDs $\lambda = 440$ nm, 1,4-dioxane:DMA, 4 : 1. B_2pro_2: bis(1,3-propanediolate)diboron; BPR: back pressure regulator; MIDA: *N*-methyliminodiacetic acid.

IIIa.[23] Oxidative quenching of the photoexcited 4CzIPN* ($E_{ox}^{1/2}$ ($PC^{\bullet+}$/PC*) = −1.18 V *vs.* SCE in CH_3CN)[14b] from glycosyl bromide **1** (E_{red} (**1a**/**1a**$^{\bullet-}$) = −2.45 V *vs.* SCE in CH_3CN)[24] can be excluded on the basis of unfavorable thermodynamics. This mechanistic pathway is supported by Stern–Volmer quenching studies, which revealed $(Me_3Si)_3SiH$ **3a** as the only reaction component able to quench the photoexcited 4CzIPN* (for details see SI, Section G).

Besides, since control experiments revealed that the reaction can also proceed in the absence of light, a further thermal initiation pathway is likely operative. In this regard, we propose that $(Me_3Si)_3SiH$ **3a** reacts with propellane **2** to give silyl radical **IIIa** and BCP radical **IV**. The latter can further react with another molecule of **3a** to give **16** and a second silyl radical **IIIa**. Then, silyl radical **IIIa** can act as a chain carrier undergoing halogen atom transfer (XAT) with glycosyl bromide **1**,[25] giving the corresponding glycosyl radical **I** and $(Me_3Si)_3SiBr$ (whose formation was confirmed by GC/MS analysis). Finally, addition of **I** to propellane **2** leads to BCP radical **II**, which subsequently reacts with **3a** to afford the BCP *C*-glycoside **4** and regenerate silyl radical **IIIa**, thereby sustaining a radical-chain. In this scenario, the side-product **15** is formed through a competitive addition reaction of silyl radical **IIIa** to propellane **2**. Although the reaction can also proceed thermally, the use of 4CzIPN provides an additional pathway to reinitiate the chain reactions once they are terminated, which explains the improved outcome when the reaction is carried out under light and in the presence of the photocatalyst.

We next investigated the mechanism for the carboboration of propellane (Scheme 3b). Following the same approach, we first demonstrated that the SOMOphile B_2pro_2 can react with propellane **2a** to give the bisboronate **17**, which likely represent the main initiation pathway for the reaction (*vide infra*). Such addition process, as well as the model carboboration reaction were completely inhibited when performed using TEMPO. In the latter case we were also able to detect by GC/MS the TEMPO adduct **18**, which proves the formation of glycosyl radicals as intermediates. Then, we interrogated the ability of B_2pro_2 to behave as a SOMOphile in the optimized reaction conditions. This diboron(4) compound is able to intercept radical species upon coordination from a Lewis base.[17b] Here, we showed that the reaction is strongly inhibited when performed using 4 Å molecular sieves, which suggest that water might activate B_2pro_2. Based on these observations, we propose a radical mechanism initiated by reaction between B_2pro_2 **3b** and propellane **2a**. Specifically, we propose that coordination of B_2pro_2 by water might lead to the formation of the active ate-complex **19** that reacts with propellane **2** giving boryl radical anion **IIIb** and BCP radical **V**.[17b,26] Addition of **V** to **19** then gives the bisboronate side-product **17**.[27] On the other hand, we speculate that the resulting boryl radical anion **IIIb** can then undergo XAT with glycosyl bromide **1**, forming glycosyl radical **I**. Finally, subsequent addition of radical **I** to propellane **2** and activated **19** leads to the desired BCP boronate **7** and restores intermediate **IIIb**, thus propagating the chain reaction.

Next, seeking to determine the origin of the α stereoselectivity, we performed DFT calculations investigating the reaction between peracetylated D-glucosyl radical **Ia** and [1.1.1]propellane **2a**. This key reactive intermediate populates three main conformations of the six-membered ring, namely the chair $^4C_1$, the inverted chair $^1C_4$, and the boat $B_{2,5}$.[3i] These conformers exhibit relative free energy values spanning a narrow range of 1.74 kcal mol^{-1}, with the $B_{2,5}$-**Ia** conformer

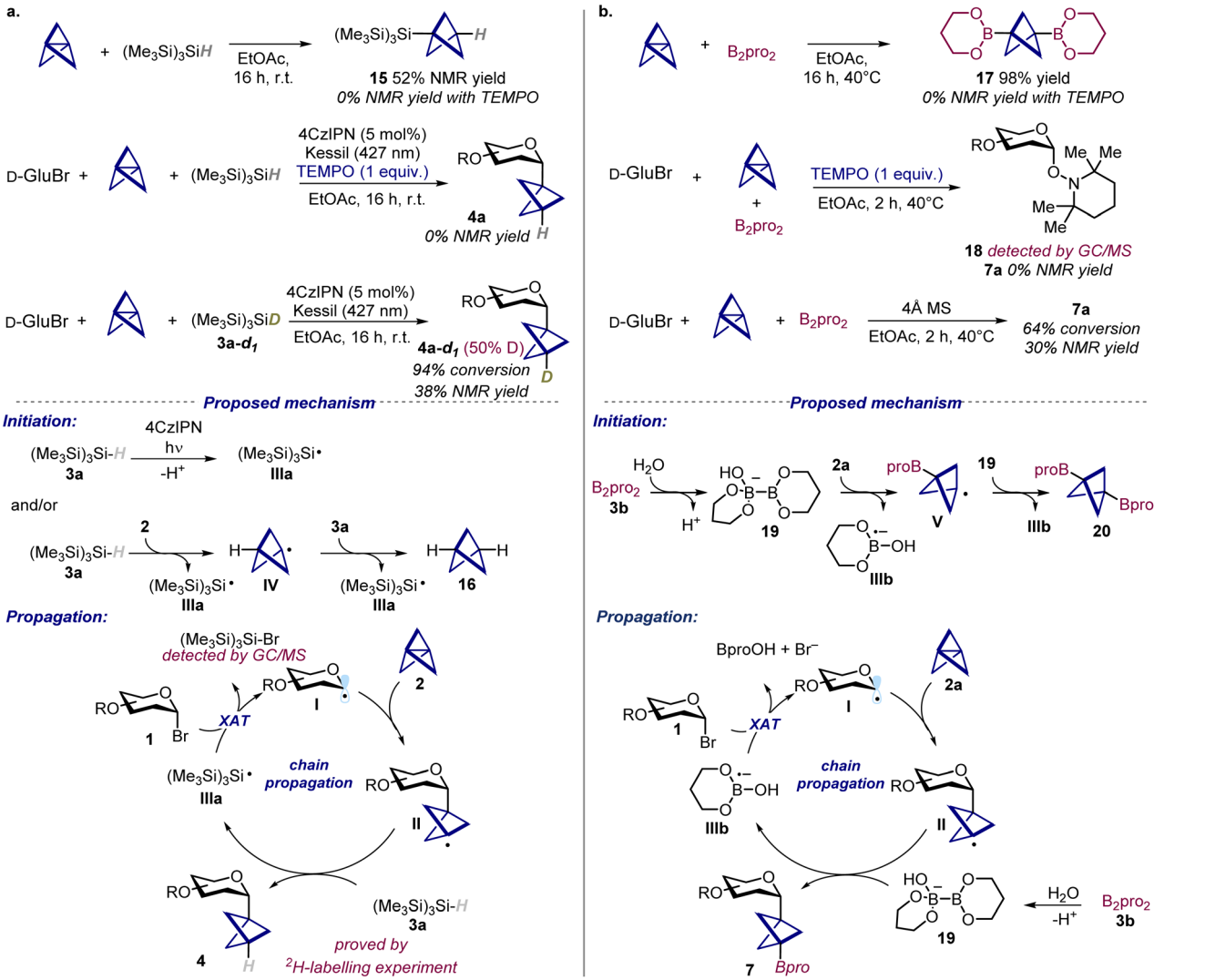

Scheme 3 Mechanistic probes and proposed mechanism for the (a) hydroglycosylation and (b) carboboration of propellanes. 4CzIPN: 1,2,3,5-tetrakis(carbazol-9-yl)-4,6-dicyanobenzene; TEMPO: 2,2,6,6-tetramethyl-1-piperidinyloxy.

being the most stable. They also show similar calculated global electrophilicity ($1.03 < \omega < 1.08$ eV), consistent with nucleophilic α-oxo carbon centered radicals.[28] The addition of **Ia** to **2a** to give BCP radical **IIa** is exergonic, with a calculated ΔG^0 of −12.4 and −14.8 kcal mol^{-1} for the α and β anomer, respectively.[29] Experimental data show the α anomer to be the favored one, suggesting that the stereoselectivity is likely determined by kinetic factors. Indeed, among the possible transition states, the lowest energy one was found to be TSα, which shows a $^4C_1$ conformation (incipient C···C bond distance of 2.297 Å, Fig. 1) while favoring α stereoselectivity ($\Delta G^{\ddagger} = +9.3$ kcal mol^{-1}).[30] For comparison, the related TSβ is associated to $\Delta G^{\ddagger} = +12.2$ kcal mol^{-1} for the pathway to β-**IIa** anomer; other TS adopting different conformations (namely $^1C_4$ or $B_{2,5}$) were found at higher energies for both α and β pathways (SI, section H). Spin density maps of both TS clearly show that the anomeric radical is partially delocalized over the endocyclic oxygen of the sugar ring, an effect that is more pronounced for the TSα. This is indicative of a better orbital overlap between the lone pair of the oxygen atom and the $\sigma^{*\ddagger}$ orbital of the incipient C–C bond.[19] Such stabilizing effect – *i.e.* the kinetic anomeric effect in radical glycosylation reactions – accounts for the α selectivity observed in the addition of glucosyl radical to [1.1.1]propellane.

An analogous DFT calculation was performed for the reaction between the peracetylated xylosyl radical **Ie** and [1.1.1] propellane **2a**, which revealed a similar trend of diastereoselectivity with the α-**IIe** anomer being the most favoured by a calculated $\Delta\Delta G^{\ddagger}$ of 1.5 kcal mol^{-1}. This value is lower than the calculated $\Delta\Delta G^{\ddagger}$ of 2.9 kcal mol^{-1} for α-**IIa**, thus being consistent with the lower stereoselectivity experimentally observed for the addition of this xylosyl derivative to [1.1.1] propellane **2a** (see SI, section H for details). These results are significant, as the stereoselectivity of glycosyl radical addition reactions has rarely been investigated by DFT calculations, and our findings align well with the available precedents.[31]

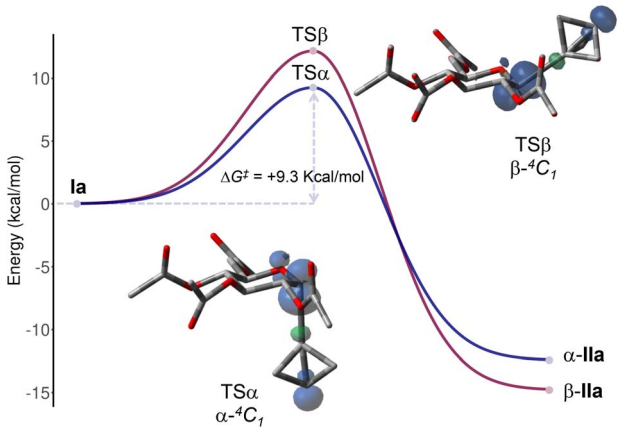

Fig. 1 Energy diagram for the addition of peracetylated glucosyl radical **Ia** to [1.1.1]propellane **2**. DFT calculation at M062X/6-311+G**//M062X/6-311+G** level of theory, including a continuum solvation model for Et_2O using the integral equation formalism variant (IEFPCM).

Conclusions

In summary, we have developed a mild radical approach for the preparation of saturated analogs of aryl *C*-glycosides. The generality of our strategy was proved in a hydroglycosylation protocol enabling the synthesis of glycosylated BCP derivatives, where the BCP moiety mimics an unsubstituted phenyl ring. By extending this reactivity to the use of diboron(4) SOMOphiles we provided access to difunctionalized glycosylated BCP boronates. This method stands out for its practicality, scalability, and synthetic versatility of the products, which enables straightforward access to a variety of BCP *C*-glycoside derivatives. Experimental and computational mechanistic studies revealed that both protocols proceed through a radical chain mechanism under a Curtin–Hammett scenario, with the stereodetermining addition of glycosyl radicals to [1.1.1]propellane being controlled by the kinetic anomeric effect. Altogether, this study introduces the replacement of planar arenes with highly three-dimensional fragments for the preparation of aryl *C*-glycoside analogues and paves the way for new developments in *C*-glycosylation chemistry.

Author contributions

GG designed the project. GG, AM, SB, PGR performed the experiments. GP performed X-ray analyses. AS performed DFT calculations. LD supervised the work and secured fundings. GG and LD wrote the manuscript with contributions from all the authors. All authors have given approval to the final version of the manuscript.

Conflicts of interest

There are no conflicts to declare.

Data availability

The data that support the findings of this study are available free of charge in the supporting information (SI). Supplementary information: includes details of experimental procedures, full characterization data, copies of NMR spectra, X-ray analysis, and DFT calculations. See DOI: **https://doi.org/10.1039/d5sc07328f**.

CCDC 2422982 contains the supplementary crystallographic data for this paper.[32]

Acknowledgements

This work was supported by the European Union H2020 research and innovation program with the ERC StG grant for SYNPHOCAT, No. 101040025 (LD); and by MUR (Ministero dell'Università) PRIN 2020927WY3_00 (LD). GG thanks MUR for a Young Researchers, Seal of Excellence fellowship funded by the European Union – NextGenerationEU (PhotoFix-Bio – C93C22007640006). SB acknowledges UniPD for a doctoral fellowship. PGR thanks CiQUS for a fellowship within the International Mobility Program 2024 framework financed by the Xunta de Galicia and the European Union.

References

1 (*a*) S. I. Elshahawi, K. A. Shaaban, M. K. Kharel and J. S. Thorson, *Chem. Soc. Rev.*, 2015, **44**, 7591–7697; (*b*) K. Kitamura, Y. Ando, T. Matsumoto and K. Suzuki, *Chem. Rev.*, 2018, **118**, 1495–1598.

2 (*a*) J. Štambaský, M. Hocek and P. Kočovský, *Chem. Rev.*, 2009, **109**, 6729–6764; (*b*) É. Bokor, S. Kun, D. Goyard, M. Tóth, J.-P. Praly, S. Vidal and L. Somsák, Two aryl *C*-glycoside derivatives, dapagliflozin and empagliflozin, are among the top 50 best-selling drugs of 2023, *Chem. Rev.*, 2017, **117**, 1687–1764, **https://www.drugdiscoverytrends.com/best-selling-pharmaceuticals-2023/**, For details, see: ; (*c*) Boehringer Ingelheim – 2023 Highlights, **https://annualreport.boehringer-ingelheim.com/2023/download/BOE_AR23_Highlights_2023_EN_safe.pdf**; (*d*) AstraZeneca Annual Report and Form 20-F Information 2024, **https://www.astrazeneca.com/content/dam/az/Investor_Relations/annual-report-2024/pdf/AstraZeneca_AR_2024.pdf**.

3 Selected reviews on the synthesis of aryl *C*-glycosides: (*a*) Y. Du, R. J. Linhardt and I. R. Vlahov, *Tetrahedron*, 1998, **54**, 9913–9959; (*b*) Y. Yang and B. Yu, *Chem. Rev.*, 2017, **117**, 12281–12356; (*c*) L.-Y. Xu, N.-L. Fan and X.-G. Hu, *Org. Biomol. Chem.*, 2020, **18**, 5095–5109; (*d*) Y. Jiang, Y. Zhang, B. C. Lee and M. J. Koh, *Angew. Chem., Int. Ed.*, 2023, **62**, e202305138; (*e*) X.-Y. Gou, X.-Y. Zhu, B.-S. Zhang and Y.-M. Liang, *Chem.–Eur. J.*, 2023, **29**, e202203351, Selected modern synthetic methods to aryl *C*-glycosides: ; (*f*) H. Gong and M. R. Gagné, *J. Am. Chem. Soc.*, 2008, **130**, 12177–12183; (*g*) S. H. Lemaire, N. Ioannis, T. Xiao, J. Li, E. Digard, C. Gozlan, R. Liu, A. Gavryushin, C. Diène, Y. Wang, V. Farina and P. Knochel, *Org. Lett.*, 2012, **14**, 1480–1483; (*h*) L. Nicolas, P. Angibaud, I. Stansfield, P. Bonnet, L. Meerpoel, S. Reymond and J. Cossy, *Angew. Chem., Int. Ed.*, 2012, **51**, 11101–11104; (*i*) L. Adak, S. Kawamura, G. Toma, T. Takenaka, K. Isozaki, H. Takaya, A. Orita, H. C. Li, T. K. M. Shing and M. Nakamura, *J. Am. Chem. Soc.*, 2017, **139**, 10693–10701; (*j*) A. Dumoulin,

J. K. Matsui, A. Gutierrez-Bonet and G. A. Molander, *Angew. Chem., Int. Ed.*, 2018, **57**, 6614–6618; (*k*) Y. Wei, B. Ben-Zvi and T. Diao, *Angew. Chem., Int. Ed.*, 2021, **60**, 9433–9438; (*l*) Z. D. Mou, J. X. Wang, X. Zhang and D. Niu, *Adv. Synth. Catal.*, 2021, **363**, 3025–3029; (*m*) C. Zhang, S.-Y. Xu, H. Zuo, X. Zhang, Q.-D. Dang and D. Niu, *Nat. Synth.*, 2023, **2**, 251–260.

4 (*a*) F. Lovering, J. Bikker and C. Humblet, *J. Med. Chem.*, 2009, **52**, 6752–6756; (*b*) T. J. Ritchie and S. J. Macdonald, *Drug Discovery Today*, 2009, **14**, 1011–1020; (*c*) F. Lovering, *MedChemComm*, 2013, **4**, 515–519.

5 (*a*) N. A. Meanwell, *J. Med. Chem.*, 2011, **54**, 2529–2591; (*b*) N. Brown, *Bioisosteres in Medicinal Chemistry*, Wiley-VCH Verlag & Co. KGaA, Weinheim, Germany, 2012; (*c*) N. A. Meanwell, *J. Agric. Food Chem.*, 2023, **71**, 18087–18122.

6 (*a*) P. K. Mykhailiuk, *Org. Biomol. Chem.*, 2019, **17**, 2839–2849; (*b*) M. A. M. Subbaiah and N. A. Meanwell, *J. Med. Chem.*, 2021, **64**, 14046–14128.

7 (*a*) R. Pellicciari, M. Raimondo, M. Marinozzi, B. Natalini, G. Costantino and C. Thomsen, *J. Med. Chem.*, 1996, **39**, 2874–2876; (*b*) A. F. Stepan, C. Subramanyam, I. V. Efremov, J. K. Dutra, T. J. O'Sullivan, K. J. DiRico, W. S. McDonald, A. Won, P. H. Dorff, C. E. Nolan, S. L. Becker, L. R. Pustilnik, D. R. Riddell, G. W. Kauffman, B. L. Kormos, L. Zhang, Y. Lu, S. H. Capetta, M. E. Green, K. Karki, E. Sibley, K. P. Atchison, A. J. Hallgren, C. E. Oborski, A. E. Robshaw, B. Sneed and C. J. O'Donnell, *J. Med. Chem.*, 2012, **55**, 3414–3424; (*c*) N. D. Measom, K. D. Down, D. J. Hirst, C. Jamieson, E. S. Manas, V. K. Patel and D. O. Somers, *ACS Med. Chem. Lett.*, 2017, **8**, 43–48; (*d*) E. G. Tse, S. D. Houston, C. M. Williams, G. P. Savage, L. M. Rendina, I. Hallyburton, M. Anderson, R. Sharma, G. S. Walker, R. S. Obach and M. H. Todd, *J. Med. Chem.*, 2020, **63**, 11585–11601.

8 (*a*) R. S. Andrews, J. J. Becker and M. R. Gagné, *Angew. Chem., Int. Ed.*, 2010, **49**, 7274–7276; (*b*) Q. Wang, B. C. Lee, T. J. Tan, Y. Jiang, W. H. Ser and M. J. Koh, *Nat. Synth.*, 2022, **1**, 967–974; (*c*) Q. Wang, Q. Sun, Y. Jiang, H. Zhang, L. Yu, C. Tian, G. Chen and M. J. Koh, *Nat. Synth.*, 2022, **1**, 235–244; (*d*) S. Xu, Y. Ping, M. Xu, G. Wu, Y. Ke, R. Miao, X. Qi and W. Kong, *Nat. Chem.*, 2024, **16**, 2054–2065; (*e*) Y. Jiang, Y. Wei, Q.-Y. Zhou, G.-Q. Sun, X.-P. Fu, N. Levin, Y. Zhang, W.-Q. Liu, N. Song, S. Mohammed, B. G. Davis and M. J. Koh, *Nature*, 2024, **631**, 319–327.

9 (*a*) K. B. Wiberg and F. H. Walker, *J. Am. Chem. Soc.*, 1982, **104**, 5239–5240; (*b*) W. Wu, J. Gu, J. Song, S. Shaik and P. C. Hiberty, *Angew. Chem., Int. Ed.*, 2009, **48**, 1407–1410; (*c*) A. J. Sterling, A. B. Durr, R. C. Smith, E. A. Anderson and F. Duarte, *Chem. Sci.*, 2020, **11**, 4895–4903, For a review on propellanes, see: ; (*d*) A. M. Dilmac, E. Spuling, A. de Meijere and S. Brase, *Angew. Chem., Int. Ed.*, 2017, **56**, 5684–5718.

10 For reviews on the use of [1.1.1]propellane in synthetic methods, see: (*a*) K. B. Wiberg and S. T. Waddell, *J. Am. Chem. Soc.*, 1990, **112**, 2194–2216; (*b*) M. Uchiyama and J. Kanazawa, *Synlett*, 2018, **30**, 1–11; (*c*) J. Turkowska, J. Durka and D. Gryko, *Chem. Commun.*, 2020, **56**, 5718–5734; (*d*) B. R. Shire and E. A. Anderson, *JACS Au*, 2023, **3**, 1539–1553; (*e*) P. Bellotti and F. Glorius, *J. Am. Chem. Soc.*, 2023, **145**, 20716–20732; (*f*) S. Cuadros, J. Paut, E. Anselmi, G. Dagousset, E. Magnier and L. Dell'Amico, *Angew. Chem., Int. Ed.*, 2024, **63**, e202317333, Selected modern approaches to the 1,3-difunctionalization of [1.1.1] propellane: ; (*g*) R. Gianatassio, J. M. Lopchuk, J. Wang, C.-M. Pan, L. R. Malins, L. Prieto, T. A. Brandt, M. R. Collins, G. M. Gallego, N. W. Sach, J. E. Spangler, H. Zhu, J. Zhu and P. S. Baran, *Science*, 2016, **351**, 241–246; (*h*) R. A. Shelp and P. J. Walsh, *Angew. Chem., Int. Ed.*, 2018, **57**, 15857–15861; (*i*) K. Schwarzer, H. Zipse, K. Karaghiosoff and P. Knochel, *Angew. Chem., Int. Ed.*, 2020, **59**, 20235–20241; (*j*) J. Kanazawa, K. Maeda and M. Uchiyama, *J. Am. Chem. Soc.*, 2017, **139**, 17791–17794; (*k*) J. H. Kim, A. Ruffoni, Y. S. S. Al-Faiyz, N. S. Sheikh and D. Leonori, *Angew. Chem., Int. Ed.*, 2020, **59**, 8225–8231; (*l*) S. Cuadros, G. Goti, G. Barison, A. Raulli, T. Bortolato, G. Pelosi, P. Costa and L. Dell'Amico, *Angew. Chem., Int. Ed.*, 2023, **62**, e202303585; (*m*) V. Ripenko, V. Sham, V. Levchenko, S. Holovchuk, D. Vysochyn, I. Klymov, D. Kyslyi, S. Veselovych, S. Zhersh, Y. Dmytriv, A. Tolmachev, I. Sadkova, I. Pishel, K. Horbatok, V. Kosach, Y. Nikandrova and P. K. Mykhailiuk, *Nat. Synth.*, 2024, **3**, 1538–1549, For rare examples of glycosyl radical addition to [1.1.1]propellane, see: ; (*n*) J. Nugent, C. Arroniz, B. R. Shire, A. J. Sterling, H. D. Pickford, M. L. J. Wong, S. J. Mansfield, D. F. J. Caputo, B. Owen, J. J. Mousseau, F. Duarte and E. A. Anderson, *ACS Catal.*, 2019, **9**, 9568–9574; (*o*) W. Dong, E. Yen-Pon, L. Li, A. Bhattacharjee, A. Jolit and G. A. Molander, *Nat. Chem.*, 2022, **14**, 1068–1077.

11 Selected book chapters and reviews on radical chemistry for carbohydrate functionalization: (*a*) A. J. Pearce, J. M. Mallet and P. Sinaÿ, in *Radicals in Organic Synthesis*, ed. P. Renaud and M. P. Sibi, WILEY-VCH Verlag GmbH, 2001, pp. 538–577, DOI: **10.1002/9783527618293.ch52**; (*b*) I. Pérez-Martín and E. Suárez, in *Encyclopedia of Radicals in Chemistry, Biology and Materials*, ed. C. Chatgilialoglu and A. Studer, John Wiley & Sons, Ltd, 2012, pp. 1131–1174; (*c*) C. E. Suh, H. M. Carder and A. E. Wendlandt, *ACS Chem. Biol.*, 2021, **16**, 1814–1828; (*d*) A. Shatskiy, E. V. Stepanova and M. D. Kärkäs, *Nat. Rev. Chem.*, 2022, **6**, 782–805; (*e*) G. Goti, *ChemCatChem*, 2022, **14**, e202200290; (*f*) W. Shang and D. Niu, *Acc. Chem. Res.*, 2023, **56**, 2473–2488, Selected references on modern synthetic methods: ; (*g*) V. Dimakos, H. Y. Su, G. E. Garrett and M. S. Taylor, *J. Am. Chem. Soc.*, 2019, **141**, 5149–5153; (*h*) Y. Wang, H. M. Carder and A. E. Wendlandt, *Nature*, 2020, **578**, 403–408; (*i*) W. Yao, G. Zhao, Y. Wu, L. Zhou, U. Mukherjee, P. Liu and M.-Y. Ngai, *J. Am. Chem. Soc.*, 2022, **144**, 3353–3359.

12 During the submission and revision process of this manuscript, Ackermann and co-workers reported an electrochemical approach to the synthesis of related bicyclo[1.1.1]pentyl *C*-glycosides: J. Liu, R. Purushothaman, F. Hinrichs, M. Surke, S. Warratz and L. Ackermann, *J. Am. Chem. Soc.*, 2025, **147**, 34813–34822, DOI: **10.1021/**

jacs.5c10732, Please note that the preprint version of our manuscripts was deposited in ChemRxiv on the 21st of March 2025 (see ChemRxiv 2025; DOI:10.26434/chemrxiv-2025-0czlj).

13 C. Chatgilialoglu, C. Ferreri, Y. Landais and V. I. Timokhin, *Chem. Rev.*, 2018, **118**, 6516–6572.

14 (*a*) N. A. Romero and D. A. Nicewicz, *Chem. Rev.*, 2016, **116**, 10075–10166; (*b*) E. Speckmeier, T. G. Fischer and K. Zeitler, *J. Am. Chem. Soc.*, 2018, **140**, 15353–15365; (*c*) T. Bortolato, S. Cuadros, G. Simionato and L. Dell'Amico, *Chem. Commun.*, 2022, **58**, 1263–1283.

15 B. Linclau, A. Arda, N. C. Reichardt, M. Sollogoub, L. Unione, S. P. Vincent and J. Jimenez-Barbero, *Chem. Soc. Rev.*, 2020, **49**, 3863–3888.

16 (*a*) N. Frank, J. Nugent, B. R. Shire, H. D. Pickford, P. Rabe, A. J. Sterling, T. Zarganes-Tzitzikas, T. Grimes, A. L. Thompson, R. C. Smith, C. J. Schofield, P. E. Brennan, F. Duarte and E. A. Anderson, *Nature*, 2022, **611**, 721–726; (*b*) T. Iida, J. Kanazawa, T. Matsunaga, K. Miyamoto, K. Hirano and M. Uchiyama, *J. Am. Chem. Soc.*, 2022, **144**, 21848–21852.

17 (*a*) E. C. Neeve, S. J. Geier, I. A. Mkhalid, S. A. Westcott and T. B. Marder, *Chem. Rev.*, 2016, **116**, 9091–9161; (*b*) F. W. Friese and A. Studer, *Chem. Sci.*, 2019, **10**, 8503–8518; (*c*) M. Kondo, J. Kanazawa, T. Ichikawa, T. Shimokawa, Y. Nagashima, K. Miyamoto and M. Uchiyama, *Angew. Chem., Int. Ed.*, 2020, **59**, 1970–1974; (*d*) M. D. VanHeyst, J. Qi, A. J. Roecker, J. M. E. Hughes, L. Cheng, Z. Zhao and J. Yin, *Org. Lett.*, 2020, **22**, 1648–1654; (*e*) Y. Yang, J. Tsien, J. M. E. Hughes, B. K. Peters, R. R. Merchant and T. Qin, *Nat. Chem.*, 2021, **13**, 950–955; (*f*) I. F. Yu, J. L. Manske, A. Dieguez-Vazquez, A. Misale, A. E. Pashenko, P. K. Mykhailiuk, S. V. Ryabukhin, D. M. Volochnyuk and J. F. Hartwig, *Nat. Chem.*, 2023, **15**, 685–693; (*g*) L. Yi, D. Kong, A. Prabhakar Kale, R. Alshehri, H. Yue, A. Gizatullin, B. Maity, R. Kancherla, L. Cavallo and M. Rueping, *Angew. Chem., Int. Ed.*, 2024, **63**, e202411961.

18 H. Yoshida, M. Seki, I. Kageyuki, I. Osaka, S. Hatano and M. Abe, *ACS Omega*, 2017, **2**, 5911–5916.

19 (*a*) H. Abe, S. Shuto and A. Matsuda, *J. Am. Chem. Soc.*, 2001, **123**, 11870–11882; (*b*) H. Abe, M. Terauchi, A. Matsuda and S. Shuto, *J. Org. Chem.*, 2003, **68**, 7439–7447.

20 (*a*) C. Sandford and V. K. Aggarwal, *Chem. Commun.*, 2017, **53**, 5481–5494; (*b*) K. Duan, X. Yan, Y. Liu and Z. Li, *Adv. Synth. Catal.*, 2018, **360**, 2781–2795.

21 (*a*) J. Wegner, S. Ceylan and A. Kirschning, *Adv. Synth. Catal.*, 2012, **354**, 17–57; (*b*) M. B. Plutschack, B. Pieber, K. Gilmore and P. H. Seeberger, *Chem. Rev.*, 2017, **117**, 11796–11893; (*c*) L. Capaldo, Z. Wen and T. Noel, *Chem. Sci.*, 2023, **14**, 4230–4247.

22 E. Wheatley, H. Melnychenko and M. Silvi, *J. Am. Chem. Soc.*, 2024, **146**, 34285–34291.

23 J. Zhu, W. C. Cui, S. Wang and Z. J. Yao, *Org. Lett.*, 2018, **20**, 3174–3178.

24 S. B. Rondinini, P. R. Mussini, F. Crippa and G. Sello, *Electrochem. Commun.*, 2000, **2**, 491–496.

25 F. Juliá, T. Constantin and D. Leonori, *Chem. Rev.*, 2022, **122**, 2292–2352.

26 (*a*) L. Capaldo, T. Noël and D. Ravelli, *Chem Catal.*, 2022, **2**, 957–966; (*b*) S. B. Thorpe, J. A. Calderone and W. L. Santos, *Org. Lett.*, 2012, **14**, 1918–1921.

27 J. R. Pinchman, C. D. Hopkins, K. D. Bunker and P. Q. Huang, WO/2018/039232, 2018.

28 (*a*) F. Parsaee, M. C. Senarathna, P. B. Kannangara, S. N. Alexander, P. D. E. Arche and E. R. Welin, *Nat. Rev. Chem.*, 2021, **5**, 486–499; (*b*) J. J. A. Garwood, A. D. Chen and D. A. Nagib, *J. Am. Chem. Soc.*, 2024, **146**, 28034–28059.

29 A conformational analysis was conducted for **I** and for both the α and β anomers of **II**, and the energies are given considering a weighted average of the conformers, according to Boltzmann distribution. While for α-**II** an almost equal contribution of $^4C_1$ and $^1C_4$ conformations was found, the β-**II** anomer is described almost exclusively by the $^4C_1$ conformation (see SI, Section H).

30 A calculated $\Delta G^{\ddagger}$ of +17 kcal mol^{-1} was reported for the addition of a nucleophilic α-amido radical to **2a**, see ref. 17g. The global electrophilicity ω of α-amido radicals is expected to range between 0.5 and 0.8 eV (see ref. 28b).

31 (*a*) L. Xia, W. Fan, X.-A. Yuan and S. Yu, *ACS Catal.*, 2021, **11**, 9397–9406; (*b*) Y. Jiang, K. Yang, Y. Wei, Q. Wang, S.-J. Li, Y. Lan and M. J. Koh, *Angew. Chem., Int. Ed.*, 2022, **61**, e202211043.

32 CCDC 2422982: Experimental Crystal Structure Determination, 2025, DOI: 10.5517/ccdc.csd.cc2mb9q0.